12. Ducray F, Criniere E, Idbaih A, Mokhtari K, Maric Y, Paris S, Navarro S, Laigle-Donadey F, Dehais C, Thilet J, Hoang-Xuan K, Delattre JY, Sanson M (2009) Alpha-internexin expression identifies 1p19q codeleted gliomas. Neurology 72:156–161
13. Ducray F, Mokhtari K, Crinière E, Idbaih A, Marie Y, Dehais C, Paris S, Carpentier C, Dieme MJ, Adam C, Hoang-Xuan K, Duyckaerts C, Delattre JY, Sanson M (2011) Diagnostic and prognostic value of alpha internexin expression in a series of 409 gliomas. Eur J Cancer 47:802–808
14. Durand K, Guillaudeau A, Pommepuy I, Mesturoux L, Chaunavel A, Gadeaud E, Porcheron M, Moreau JJ, Labrousse F (2011) Alpha-internexin in gliomas, relationship with histological type and 1p, 19q, 10p and 10q status. J Clin Pathol 64:793–801
15. Mokhtari K, Ducray F, Kros JM, Gorlia T, Idbaih A, Taphoom M, Wesseling P, Hoang-Xuan K, van den Bent M, sanson M (2011) Alpha-internexin expression predicts outcome IN anaplastic oligodendroglial tumors and may positively impact the efficacy of chemotherapy. Cancer 117:3014–3026
16. Preusser M, Wohrer A, Stary S, Hoftberger R, Streubel B, Hainfellner JA (2011) Value and limitations of immunohistochemistry and gene sequencing for detection of the IDH1-R132H mutation in diffuse glioma biopsy specimens. J Neuropathol Exp Neurol 70:715–723
17. Sonoda Y, Yokosawa M, Saito R, Kanamori M, Yamashita Y, Kumabe T, Watanabe M, Tominaga T (2010) O6-Methylguanine DNA methyltransferase determined by promoter hypermethylation and immunohistochemical expression is correlated with progression-free survival in patients with glioblastoma. Int J Clin Oncol 15:352–358
18. Christman M, Naegel G, Hom S, Krhan U, Wiewroft D, Sommer C, Kaima B (2010) MGMT activity, promoter methylation and immunohistochemistry of pretreatment and recurrent malignant gliomas: a comparative study on astrocytoma and glioblastoma. Int J Cancer 127:2106–2118
19. Momota H, narita Y, Matsushita Y, Miyakita Y, Shibui S (2010) p53 abnormality and tumor invasion in patients with malignant astrocytoma. Brain Tumor Pathol 27:95–101
20. Pardo FS, Hsu DW, Zeheb R, Efird JT, Okurief PG, Malkin DM (2004) Mutant, wild type, or overall p53 expression: freedom from clinical progression in tumours of astrocytic lineage. Br J Cancer 91:1678–1686
21. Kloosterhof NK, Bralte LB, Dubbink HJ, French PJ, van den Bent M (2011) Isocitrate dehydrogenase-1 mutations: a fundamentally new understanding of diffuse glioma? Lancet Oncol 12:83–91
22. Sanson M, Marie Y, Paris S, Idbaih A, Laffaire J, Ducray F, El Hallani S, Boisseller B, Mokhtari K, Hoang-Xuan K, Delattre JY (2009) Isocitrate dehydrogenase 1 codon 132 mutation is an important prognostic biomarker in gliomas. J Clin Oncol 27:4150–4154
23. van den Bent MJ, Dubbink HJ, Marie Y, Brandes AA, Taphoom MJ, Wesseling P, Frenay M, Tijssen CC, Lacombe D, Idbaih A, van Marion R, Kros JM, Dinjens WN, Gorlia T, Sanson M (2010) IDH1 and IDH2 mutations are prognostic but not predictive for outcome in anaplastic oligodendroglial tumors: a report of the European organization for research and treatment of cancer brain tumor group. Clin Cancer Res 16:1597–1604
24. Hartmann C, Hentschel B, Wick W, Capper D, Felsberg J, Simon M, Westphal M, Schackert G, Meyermann R, Pietsch T, Reifenerger G, Weller M, Loeffler M, von Deimling A (2010) Patients with IDH1 wild type anaplastic astrocytomas exhibit worse prognosis than IDH1-mutated glioblastomas, and IDH1 mutation status accounts for the unfavorable prognostic effect of higher age: implications for classification of gliomas. Acta Neuropathol 120:707–718
25. Gupta R, Webb-Myers R, Flanagan S, Buckland ME (2011) Isocitrate dehydrogenase mutations in diffuse gliomas: clinical and aetiological implications. J Clin Pathol 64:835–844 (July 12 [Epub ahead of print])
26. Capper D, Weibert S, Balss J, Habel A, Meyer J, Jager D, Ackermann U, Tessmer C, Korshunov A, Zentgraf H, Hartmann C (2010) Characterization of R132H mutation-specific IDH1 antibody binding in brain tumors. Brain Pathol 20:245–254
27. Dubbink HJ, Taal W, van Marion R, Kros JM, van Heuvel I, Bromberg JE, Zonnenberg BA, Zonnenberg CB, Postma TJ, Gijtenbeek JM, Boogerd W, Groenendijk FH, Smitt PA, Dinjens WN, van den Bent MJ (2009) IDH1 mutations in astrocytomas predict survival but not response to temozolomide. Neurology 73:1792–1795
28. Thon N, Eigenbrod S, Kreth S, Lutz J, Tonn JC, Kretzschmar H, Peraud A, Kreth FW (2011) IDH1 mutations in grade II astrocytomas are associated with unfavorable progression-free survival and prolonged postrecurrence survival. Cancer 118(2): 452–460
29. Kim YH, Nobusawa S, Mittelbronn M, Paulus W, Brokinkel B, Keyvani K, Sure U, Wrede K, Nakazato Y, Tanaka Y, Vital A, Mariani L, Stawaski R, Watanabe T, de Girolami U, Kleihues P, Ohgaki H (2010) Molecular classification of low-grade diffuse glioma. Am J Pathol 177:2708–2714
30. Houillier C, Wang X, Kaloshi G, Mokhtari K, Guilevin R, Laffaire J, Paris S, Boisselier B, Idbah A, Laigle-Donadey F, Sanson M, Delattre JY (2010) IDH1 or IDH2 mutations predict longer survival and response to temozlomide in low-grade gliomas. Neurology 75:1560–1566
31. Pignatti F, van den Bent M, Curran D, Debruyne C, Sylvester R, Therasse P, Afra D, Cornu P, Bolla M, Vecht C, Karim AB, European Organization for Research and Treatment of Cancer Brain Tumor Cooperative Group, European Organization for Research and Treatment of Cancer Radiotherapy Cooperative Group (2002) Prognostic factors for survival in adult patients with cerebral low-grade glioma. J Clin Oncol 20:2076–2084
32. Metellus P, Coulibaly B, Colin C, de Paula AM, Vasiljevic A, Taieb D, Barlier A, Boisselier B, Mokhatari K, Wang XW, Loundou A, Chapon F, Pineau S, Ouafik L, Chinot O, Figarella-Branger D (2010) Absence of IDH mutation identifies a novel radiological and molecular subtype of WHO grade II gliomas with dismal prognosis. Acta Neuropathol 120:719–729
33. Baas IO, Mulder JW, Offerhaus GJ, Vogelstein B, Hamilton SR (1994) An evaluation of six antibodies for immunohistochemistry of mutant p53 gene product in archival colorectal neoplasms. J Pathol 172:5–12
34. Ohgaki H, Kleihues P (2009) Genetic alterations and signaling pathway in the evolution of gliomas. Cancer Sci 100:2235–2241
35. Birner P, Toumangelova-Uzeir K, Natchev S, Guentchev M (2011) Expression of mutated isocitrate dehydrogenase-1 in gliomas is associated with p53 and EGFR expression. Folia Neuropathol 49:88–93
36. Kurtkaya-Yapicier O, Scheithauer BW, Hebrink D, James CD (2002) p53 in nonneoplastic central nervous system lesions: an immunohistochemical and genetic sequencing study. Neurosurgery 51:1246–1254
37. Yip S, Butterfield YS, Morozova O, Chittaranjan S, Blough MD, An J, Birol I, Chesnelong C, Chiu R, Chuah E, Corbett R, Docking R, Firme M, Hirst M, Jackman S, Karsan A, Li H, Louis DN, Maslova A, Moore R, Moradian A, Mungall KL, Perizzolo M, Qian J, Roldan G, Smith EE, Tamura-Wells J, Thiessen N, Varhol R, Weiss S, Wu W, Young S, Zhao Y, Mungall AJ, Jones SJ, Morin GB, Chan JA, Cairncross JG, Marra MA (2012) Concurrent CIC mutations, IDH mutations, and 1p/19q loss distinguish oligodendrogliomas from other cancers. J Pathol 226(1):7–16

38. Precusser M, Charles JR, Felsberg J, Reifenberger G, Hanou MF, Diserens AC, Stupp R, Gorlia T, Marosi C, Heizl H, Hainfellner JA, Hegi M (2008) Anti-O6-methylguanine-methytransferase (MGMT) immunohistochemistry in glioblastoma multiforme observer variability and lack of association with patient survival impede its use as clinical biomarker. Brain Pathol 18:520–532

39. Cao VT, Jung TY, Jung S, Jin SG, Moon KS, Kim IY, Kang SS, Park CS, Lee KH, Chae HJ (2009) The correlation and prognostic significance of MGMT promoter methylation and MGMT protein in glioblastoma. Neurosurgery 65:866–875

Japanese Journal of Clinical Oncology Advance Access published July 27, 2012

JJCO Japanese Journal of Clinical Oncology

Jpn J Clin Oncol 2012
doi:10.1093/jjco/hys121

Original Article

Phase II Study of Single-agent Bevacizumab in Japanese Patients with Recurrent Malignant Glioma†

Motoo Nagane[1,*], Ryo Nishikawa[2], Yoshitaka Narita[3], Hiroyuki Kobayashi[4], Shingo Takano[5], Nobusada Shinoura[6], Tomokazu Aoki[7], Kazuhiko Sugiyama[8], Junichi Kuratsu[9], Yoshihiro Muragaki[10], Yutaka Sawamura[11] and Masao Matsutani[2]

[1]Department of Neurosurgery, Kyorin University Faculty of Medicine, Tokyo, [2]Department of Neuro-Oncology/Neurosurgery, International Medical Center, Saitama Medical University, Saitama, [3]Department of Neurosurgery and Neuro-Oncology, National Cancer Center Hospital, Tokyo, [4]Department of Neurosurgery, Graduate School of Medicine, Hokkaido University, Hokkaido, [5]Department of Neurosurgery, Graduate School of Human Science, University of Tsukuba, Ibaraki, [6]Department of Neurosurgery, Komagome Metropolitan Hospital, Tokyo, [7]Department of Neurosurgery, Kitano Hospital, Osaka, [8]Depatment of Neurosurgery, Hiroshima University School of Medicine, Hiroshima, [9]Department of Neurosurgery, Kumamoto University Faculty of Life Sciences, Kumamoto, [10]Faculty of Advanced Techno-Surgery Graduate School of Medicine, Tokyo Women's Medical University, Tokyo and [11]Sawamura Neurosurgery Clinic, Hokkaido, Japan

*For reprints and all correspondence: Motoo Nagane, Department of Neurosurgery, Kyorin University Faculty of Medicine, 6-20-2 Shinkawa, Mitaka, Tokyo 181-8611, Japan. E-mail: nagane-nsu@umin.ac.jp

†These data were previously presented at the 2011 European Multidisciplinary Cancer Congress, jointly organized by the European CanCer Organisation (ECCO) and European Society for Medical Oncology (ESMO), Stockholm, Sweden, 23–27 September 2011 and the 2011 Society for Neuro-Oncology, CA, USA, 17–20 November 2011.

Received April 18, 2012; accepted July 1, 2012

Objective: This single-arm, open-label, Phase II study evaluated the efficacy and safety of single-agent bevacizumab, a monoclonal antibody against vascular endothelial growth factor, in Japanese patients with recurrent malignant glioma.

Methods: Patients with histologically confirmed, measurable glioblastoma or World Health Organization Grade III glioma, previously treated with temozolomide plus radiotherapy, received 10 mg/kg bevacizumab intravenous infusion every 2 weeks. The primary endpoint was 6-month progression-free survival in the patients with recurrent glioblastoma.

Results: Of the 31 patients enrolled, 29 (93.5%) had glioblastoma and 2 (6.5%) had Grade III glioma. Eleven (35.5%) patients were receiving corticosteroids at baseline; 17 (54.8%) and 14 (45.2%) patients had experienced one or two relapses, respectively. The 6-month progression-free survival rate in the 29 patients with recurrent glioblastoma was 33.9% (90% confidence interval, 19.2–48.5) and the median progression-free survival was 3.3 months. The 1-year survival rate was 34.5% with a median overall survival of 10.5 months. There were eight responders (all partial responses) giving an objective response rate of 27.6%. The disease control rate was 79.3%. Eight of the 11 patients taking corticosteroids at baseline reduced their dose or discontinued corticosteroids during the study. Bevacizumab was well-tolerated and Grade $\geq$3 adverse events of special interest to bevacizumab were as follows: hypertension [3 (9.7%) patients], congestive heart failure [1 (3.2%) patient] and venous thromboembolism [1 (3.2%) patient]. One asymptomatic Grade 1 cerebral hemorrhage was observed, which resolved without treatment.

Conclusion: Single-agent bevacizumab provides clinical benefit for Japanese patients with recurrent glioblastoma.

Key words: bevacizumab – glioblastoma – Asian continental ancestry group – Phase II – glioma

INTRODUCTION

Glioblastoma (GBM) is the most aggressive form of primary malignant brain tumor and the prognosis for patients with GBM is poor (1,2); the majority will relapse following initial treatment and $<10\%$ are alive at 5 years (3). The standard treatment for patients with newly diagnosed GBM is surgical resection followed by temozolomide (TMZ) and radiotherapy (RT), and then adjuvant TMZ alone (Stupp regimen) (4). Treatment options for patients with recurrent GBM, however, are limited and include repeat resection, RT and systemic chemotherapy, such as TMZ, nitrosoureas, platinum-based regimens (carboplatin, cisplatin), cyclophosphamide, irinotecan and etoposide, and appropriate treatment will depend on the patient and tumor characteristics (5). Currently there is no standard therapy for recurrent GBM and the estimated 6-month progression-free survival (PFS) rate for patients with recurrent disease is 9–28% (6–11) with a 1-year survival rate of 14–32% (6–8,10,11). Therefore, new treatment strategies for recurrent GBM are needed.

An alternative therapeutic approach is the inhibition of angiogenesis through the vascular endothelial growth factor (VEGF), a key regulator of angiogenesis. High levels of VEGF are expressed in GBM cells (12,13), and hypoxia and acidosis, conditions commonly seen in solid tumors, upregulate VEGF expression in glioma cells *in vivo* (14). In a mouse model, monoclonal antibodies to VEGF have been shown to inhibit the growth of the C6 glioma (15). Bevacizumab (Avastin®) is a monoclonal antibody that inhibits VEGF and is currently approved for a range of metastatic cancers (colorectal, non-small-cell lung, breast, ovarian cancer and renal cancers) (16–19) as well as for use in adults with recurrent GBM in many countries including the USA (20,21). Early Phase II studies in patients with recurrent GBM showed the efficacy of bevacizumab in combination with irinotecan (22,23). Subsequently, two Phase II studies (24–26) showed the efficacy of single-agent bevacizumab with regard to response rates and 6-month PFS in patients with recurrent GBM who had previously received RT and TMZ. These two studies formed the basis of bevacizumab's approval by the Food and Drug Administration (FDA) in 2009. Moreover, other studies have shown the efficacy of bevacizumab in recurrent GBM whether given as a single agent (27) or combined with irinotecan (28,29) and other chemotherapies, such as etoposide, carboplatin and fotemustine (30–33). Given the current evidence for bevacizumab in recurrent GBM in Western patient populations, we investigated the efficacy and safety of single-agent bevacizumab in a Phase II, single-arm, open-label study (JO22506) in Japanese patients with recurrent malignant glioma.

PATIENTS AND METHODS

The trial was carried out in accordance with the principles of Good Clinical Practice and the Declaration of Helsinki; all patients provided written informed consent prior to any study-related procedure. The protocol was approved by the institutional review boards of all participating centers. The study was registered with the Japan Pharmaceutical Information Center-Clinical Trials Information (JapicCTI), trial number: JapicCTI-090841.

Eligibility

Eligible patients were aged ≥ 20 years with histologically confirmed GBM or World Health Organization (WHO) Grade III glioma, the latter being reconfirmed at the time of surgery for recurrent glioma. Patients had magnetic resonance imaging (MRI)-confirmed disease recurrence or progression with measurable lesions within 2 weeks prior to the first study treatment and no evidence of acute or subacute cerebral hemorrhage and had received prior TMZ and RT for malignant glioma. Other key inclusion criteria were a Karnofsky performance status (KPS) $\geq 70\%$, a life expectancy of ≥ 3 months and adequate hematologic, renal and hepatic function (i.e. absolute neutrophil count $\geq 1500/mm^3$, platelet count $\geq 100\,000/mm^3$, hemoglobin ≥ 10 g/dl, bilirubin $\leq 1.5 \times$ the upper limit of normal (ULN), aspartate aminotransferase and alanine aminotransferase $\leq 2.5 \times$ ULN, serum creatinine $\leq 1.25 \times$ ULN). The following minimum intervals of time must have elapsed between the termination of therapies and the start of bevacizumab treatment: RT 8 weeks; surgical therapy and incisional biopsy 4 weeks; endocrine therapy and immunotherapy 3 weeks; post-traumatic intervention (except for patients with non-healing wounds) 2 weeks; transfusion and the use of hematopoietic growth factors 2 weeks; aspiration cytology and needle biopsy 1 week; nitrosoureas 6 weeks, procarbazine 3 weeks, vincristine 2 weeks and other chemotherapies 4 weeks and other investigational new drugs and unapproved drugs 4 weeks. Patients were excluded if they had: prior treatment with bevacizumab; a history of treatment with carmustine wafers, stereotactic radiotherapy, proton therapy or neutron capture therapy; ≥ 3 prior regimens for malignant glioma and inadequately controlled hypertension, heart disease, symptomatic cerebrovascular disorder, gastrointestinal (GI) perforation, fistula or abdominal abscess within 6 months prior to enrollment.

Study Design

This single-arm, open-label, Phase II study was conducted at 10 sites in Japan. One cycle of treatment was defined as one

bevacizumab infusion administered on Day 1 every 2 weeks. Eligible patients received 10 mg/kg bevacizumab as an intravenous infusion administered over 90 ($\pm$ 15) min on Day 1 of each cycle, which could be reduced to 30 min by Cycle 3 if no infusion reactions occurred. Treatment continued until disease progression (PD) or unacceptable toxicity. Bevacizumab doses were adjusted only for changes of $\geq$10% in body weight during the study. In the event of unacceptable toxicity, bevacizumab treatment was delayed or discontinued according to pre-specified criteria. Bevacizumab was discontinued if multiple adverse events (AEs) fulfilling the pre-specified delay or discontinuation criteria occurred in the same cycle, if cerebral hemorrhage occurred and if delayed treatment could not be restarted within 6 weeks of the last bevacizumab infusion. Patients who discontinued bevacizumab were followed for survival. Bevacizumab was provided by Chugai Pharmaceutical Co. Ltd (Tokyo, Japan).

Assessment of Efficacy

The primary endpoint was 6-month PFS in patients with recurrent GBM only. Six-month PFS was defined as the percentage of patients who remained alive and progression free at 24 weeks and was chosen based on published evidence demonstrating its extrapolation to the overall survival (OS) (6,7). Secondary efficacy endpoints included the 1-year survival, PFS, objective response rate (ORR), duration of response (DOR), OS and disease control rate (DCR).

Efficacy was assessed every third cycle (i.e. Cycles 3, 6, 9 etc.). Progression and objective response were determined by comprehensive evaluation of the results from MRI scans, corticosteroid dose assessment and neurocognitive function assessment. They were assessed by an independent radiology facility (IRF) by reference to Macdonald's Criteria (34). Response was classified according to the following categories: complete response (CR), partial response (PR), no change (NC) and PD. Confirmation of the response was determined on two consecutive assessments $\geq$4 weeks apart: patients who were determined as having CR or PR were defined as responders; patients who were determined as having NC or PD were defined as non-responders.

Percentage tumor shrinkage was also assessed and was calculated from the sum of the products of the diameters (SPD) at baseline and the smallest SPD after baseline.

Assessment of Safety

AEs were assessed throughout the study and were graded according to the Common Terminology Criteria for AEs version 3.0 (35). Body weight, vital signs and laboratory tests were assessed prior to the start of each cycle.

Statistical Methods

The efficacy analysis population comprised all patients with recurrent GBM. Patients with Grade III glioma were also evaluated for efficacy, but were not included in the primary analysis. All patients were evaluated for safety.

Statistical analysis to detect a 6-month PFS of 35% was established based on data from previous studies [BRAIN study [24] (42.6% with bevacizumab monotherapy) and the NCI-06-C-0064E study [26] (29% with bevacizumab monotherapy)], in which a 15% threshold for 6-month PFS was defined. Under these conditions, 28 patients with recurrent GBM would provide at least 80% power to detect a 20% increase in 6-month PFS from 15 to 35% at the 5% one-sided significance level. Assuming that other WHO Grade III glioma patients would be enrolled, the overall target sample size was 32 patients.

The 6-month PFS, median PFS, OS and DOR were calculated by the Kaplan–Meier method and confidence intervals (CIs) calculated by Greenwood's formula (36). Exact binomial CIs were used for estimated intervals for response rates.

RESULTS

Patients

Between August 2009 and July 2010, 31 patients were enrolled, 29 of whom were included in the efficacy analysis population. All enrolled patients received a median of 6 bevacizumab doses. Treatment was discontinued in a total of 25 patients: 23 (74.2%) due to PD; 2 (6.5%) due to AEs. Efficacy and safety analyses, except for OS, were performed after an observation period of $\geq$6 months (data cut-off 7 January 2011); the OS analyses, which included data collected through to 22 August 2011, were performed after all enrolled patients had been observed for $\geq$1 year.

Demographic Data

The majority of patients (29; 93.5%) had GBM; 2 (6.5%) had Grade III glioma (Table 1). The median age was 54.0 years (range: 23–72); 10 (32.3%) patients were aged $\geq$65 years. The percentage of males to females was well balanced. Patients were in relatively good health with 61.3% having a KPS of 90–100, and 64.5% of patients not receiving corticosteroids at the start of the study. Similar numbers of patients had experienced 1 [17 (54.8%)] or 2 [14 (45.2%)] relapses.

Efficacy Outcomes

At the time the PFS and OS analyses were performed, 22 PD events and 21 death events had been reported in the 29 patients with recurrent GBM. The 6-month PFS rate in the 29 patients with recurrent GBM (primary endpoint) was 33.9% (90% CI, 19.2–48.5), and this exceeded the 15% threshold ($P = 0.0170$). Kaplan–Meier estimates of PFS showed a steady decline over the initial 6 months with a median PFS of 3.3 months (95% CI 2.8–6.0) (Fig. 1). The 1-year survival rate for these patients was 34.5% (90%

Table 1. Demographic and baseline disease characteristics

Parameter	All patients ($n = 31$)	GBM ($n = 29$)	WHO Grade III ($n = 2$)[a]
Median age, years (range)	54.0 (23–72)	57.0 (23–72)	32.5 (30–35)
Age groups in years, *n* (%)			
≤40	6 (19.4)	4 (13.8)	2 (100)
41–64	15 (48.4)	15 (51.7)	0 (0.0)
≥65	10 (32.3)	10 (34.5)	0 (0.0)
Gender, *n* (%)			
Male	16 (51.6)	14 (48.3)	2 (100)
Female	15 (48.4)	15 (51.7)	0 (0.0)
KPS, *n* (%)			
70–80	12 (38.7)	12 (41.4)	0 (0.0)
90–100	19 (61.3)	17 (58.6)	2 (100)
Relapse/progression status, *n* (%)			
First	17 (54.8)	17 (58.6)	0 (0.0)
Second	14 (45.2)	12 (41.4)	2 (100)
Duration of malignant glioma[b]			
Median, months (range)	15.2 (5.6–213.3)	15.0 (5.6–213.3)	46.8 (27.8–65.8)
Time from RT to bevacizumab[c]			
Median, months (range)	13.2 (3.8–209.6)	13.1 (3.8–209.6)	44.8 (25.5–64.1)
Corticosteroid use at baseline, *n* (%)			
Yes	11 (35.5)	10 (34.5)	1 (50.0)
No	20 (64.5)	19 (65.5)	1 (50.0)

GBM, glioblastoma; WHO, World Health Organization; KPS, Karnofsky performance status; RT, radiotherapy; q2w, every 2 weeks.
[a]One patient had anaplastic astrocytoma and one patient had anaplastic oligoastrocytoma.
[b]Time since the initial diagnosis of malignant glioma.
[c]Time from the last RT to the first dose of bevacizumab.

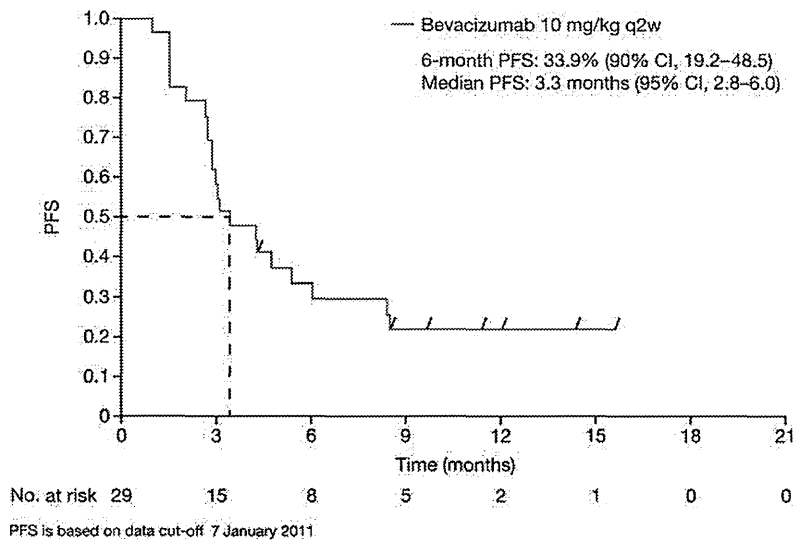

Figure 1. Progression-free survival determined by independent radiology facility in patients with recurrent glioblastoma (GBM).

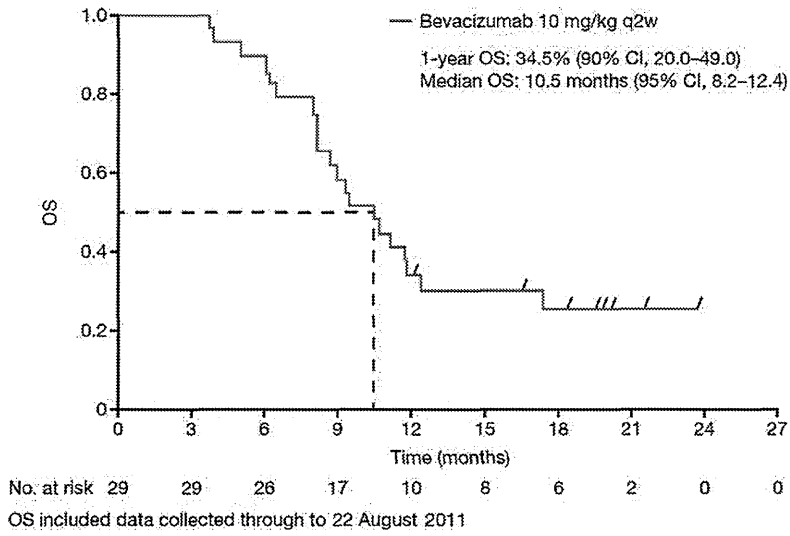

Figure 2. Overall survival in patients with recurrent GBM.

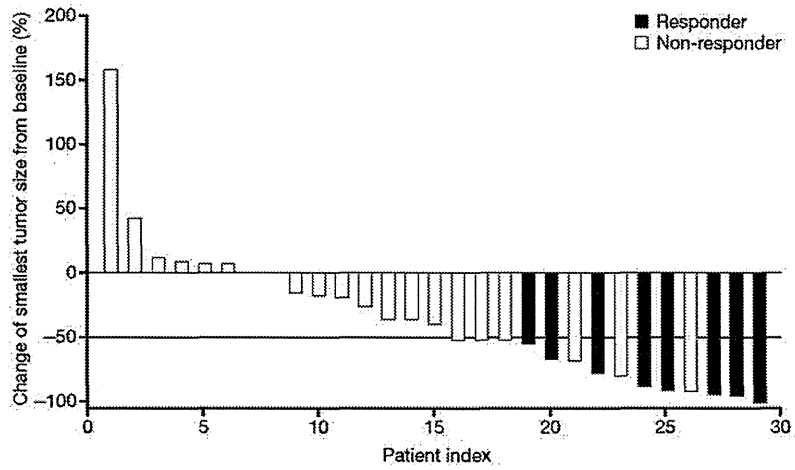

Figure 3. Waterfall plot showing the change in tumor size from baseline.

CI 20.0–49.0) with a median OS of 10.5 months (95% CI 8.2–12.4) (Fig. 2).

There were eight responders (all PR) with an ORR of 27.6% (95% CI 12.7–47.2). The DCR (0 CR + 8 PR + 15 NC) was 79.3% (95% CI 60.3–92.0). The two patients with WHO Grade III glioma completed one and two cycles of treatment, respectively; both experienced PD. Twenty-one patients (72.4%) with recurrent GBM experienced tumor shrinkage during the treatment period (Fig. 3), including 13 patients who were classified as non-responders. Of the 11 patients who were taking corticosteroids at baseline, dose reductions or discontinuation of corticosteroids occurred in 8 patients.

Efficacy endpoints were investigated in different patient subgroups (Table 2). Patients who were aged <50 years or <65 years, male, with a high KPS (90–100), on their first treatment relapse, not receiving corticosteroid therapy at baseline, or having been diagnosed with GBM at the initial diagnosis of malignant glioma, appeared to have a better response to bevacizumab treatment than other patients.

Safety Outcomes

All 31 patients experienced AEs with a total of 220 AEs reported during the study (Table 3). Serious AEs occurred in 11 (35.5%) patients, the most common being convulsion [2 (6.5%) patients]. Two (6.5%) patients discontinued the study due to AEs: one patient experienced a Grade 1 cerebral hemorrhage, and one patient had Grade 2 neutropenia that meant re-treatment within 6 weeks was not possible. A total of 13 (41.9%) patients experienced an AE of Grade ≥3, the most common being hypertension [3 (9.7%) patients]. No

Table 2. Six-month PFS and ORR by subgroup in patients with recurrent GBM

Variable	Bevacizumab 10 mg/kg, q2w ($n = 29$)	
	Six-month PFS, % (95% CI)	ORR, %
Age, years		
<65 ($n = 19$)	42.1 (19.9–64.3)	36.8
≥65 ($n = 10$)	15.0 (0.0–40.2)	10.0
Age, years		
<50 ($n = 11$)	45.5 (16.0–74.9)	45.5
≥50 ($n = 18$)	26.7 (5.7–47.6)	16.7
Gender		
Female ($n = 15$)	24.0 (1.3–46.7)	20.0
Male ($n = 14$)	42.9 (16.9–68.8)	35.7
KPS		
70–80 ($n = 12$)	16.7 (0.0–37.8)	8.3
90–100 ($n = 17$)	47.1 (23.3–70.8)	41.2
Relapse/progression status		
First ($n = 17$)	46.3 (22.3–70.4)	35.3
Second ($n = 12$)	16.7 (0.0–37.8)	16.7
Corticosteroid use at baseline		
Yes ($n = 10$)	20.0 (0.0–44.8)	10.0
No ($n = 19$)	42.1 (19.9–64.3)	36.8
Initial diagnosis of malignant glioma by site		
GBM ($n = 23$)	43.0 (22.6–63.5)	34.8
Other ($n = 6$)	0.0 (0.0–0.0)	0.0

PFS, progression-free survival; ORR, objective response rate; CI, confidence interval.

Table 3. Adverse events ≥Grade 3 and adverse events of special interest to bevacizumab

Patients, *n* (%)	Bevacizumab 10 mg/kg, q2w ($n = 31$)	
	All grade	Grade ≥3
Total patients with at least one AE	31 (100.0)	13 (41.9)
Irregular menstruation	3 (9.7)	2 (6.5)
Pyrexia	7 (22.6)	1 (3.2)
Convulsion	3 (9.7)	1 (3.2)
Depressed level of consciousness	1 (3.2)	1 (3.2)
Hydrocephalus	1 (3.2)	1 (3.2)
Increased intracranial pressure	1 (3.2)	1 (3.2)
Brain edema	1 (3.2)	1 (3.2)
Hemiplegia	1 (3.2)	1 (3.2)
Appendicitis	1 (3.2)	1 (3.2)
Urinary tract infection	1 (3.2)	1 (3.2)
Delirium	1 (3.2)	1 (3.2)
Neutropenia	5 (16.1)	1 (3.2)
Leukopenia	5 (16.1)	1 (3.2)
AEs of special interest to bevacizumab	22 (71.0)	5 (16.1)
Proteinuria	13 (41.9)	—
Hemorrhage[a,b]	10 (32.3)	—
Hypertension	10 (32.3)	3 (9.7)
Congestive heart failure	1 (3.2)	1 (3.2)
Venous thromboembolism	1 (3.2)	1 (3.2)

AE, adverse event.
[a]All events were Grade 1.
[b]Includes: epistaxis, gingival bleeding, conjunctival hemorrhage, infusion site hemorrhage, blood urine present, cerebral hemorrhage, hemorrhage subcutaneous, metrorrhagia.

incidence of Grade 4 or 5 hypertension was observed. One patient died of brain edema (Grade 5 AE), which was considered by the investigator to be related to PD with no causal relationship with bevacizumab treatment.

A total of 22 (71.0%) patients experienced AEs of special interest to bevacizumab, comprising proteinuria, hemorrhage, hypertension, congestive heart failure and venous thromboembolism (Table 3). One Grade 1 cerebral hemorrhage was observed on MRI; this was asymptomatic and resolved without treatment. Five (16.1%) patients had Grade 3 AEs of special interest to bevacizumab, comprising congestive heart failure [1 (3.2%) patient], venous thromboembolism [1 (3.2%) patient] and hypertension [3 (9.7%) patients]. No patients reported the other AEs of special interest to bevacizumab, i.e. reversible posterior leukoencephalopathy syndrome, wound-healing complications, GI perforation or fistulae.

Abnormal laboratory results were reported in 74.2% of patients. The most common abnormal laboratory result was proteinuria, which was reported in 41.9% of patients. Abnormal laboratory results classed as ≥Grade 3 were observed in two patients, reported as neutropenia and leukopenia.

DISCUSSION

This is the first clinical trial to investigate the safety and efficacy of single-agent bevacizumab in Japanese patients with recurrent GBM. Our data demonstrated that single-agent bevacizumab 10 mg/kg was effective in terms of the 6-month PFS, ORR, OS and 1-year survival, and was well tolerated in this Japanese population. In addition, the majority [21 (72.4%)] of patients with recurrent GBM experienced some tumor shrinkage during the treatment period.

The observed 6-month PFS of 33.9% and ORR of 27.6% seen in our study were more favorable than previous published data. These data are numerically higher than those reported for other studies with other chemotherapy and/or RT regimens (6-month PFS 9–21% and ORR 4–9%)

(6,7,10,11,37), and comparable with those reported for single-agent bevacizumab (42.6 and 28.2% for 6-month PFS and ORR, respectively) (24).

The use of Macdonald's Criteria was standard when this study was initiated; however, subsequently the Response Assessment in Neuro-Oncology (RANO) Working Group has recommended assessing MRI T2-weighted or fluid-attenuated inversion recovery (FLAIR) of non-enhancing lesions in addition to enhancing lesions (38). As the Macdonald's Criteria only assess contrast-enhancing lesions, there are risks that pseudoprogression and pseudoresponses may be considered real treatment effects. In our study an IRF assessed the changes in the T2/FLAIR signal, which was not included in the primary response evaluation based on Macdonald's Criteria. No significant increase in the T2/FLAIR signal was confirmed in the eight responders for the DOR, and seven out of eight responders exhibited $\geq$6 months' DOR. Based on these results, we are convinced that the objective response seen in our study is not a pseudoresponse.

Of the 29 GBM patients treated, 21 exhibited tumor shrinkage, including 8 patients who had a PR and 13 'non-responders' who were determined as NC or PD but exhibited some benefit with bevacizumab that was not captured by the response criteria; the maximum percentage of tumor shrinkage in 6 patients was >50%. The apparent discrepancy between the number of responders and the number of patients with tumor shrinkage is likely to be due to the ways in which the endpoints are calculated. The percentage of tumor shrinkage is calculated from the SPD at baseline and the smallest SPD after baseline, whereas for a patient to be classed as a responder, there had to be a decrease in tumor volume by $\geq$50% in the product of two diameters according to confirmation MRI performed $\geq$4 weeks after an observed response, as well as no increase in corticosteroid dosage and no neurologic deterioration. This leads to the difference between the number of patients with tumor shrinkage and the number of responders.

The 6-month PFS and ORR results were better for patients who had experienced one relapse than for those who had experienced two relapses, which is the same as a previously published observation (24). In addition, in our study bevacizumab improved the 6-month PFS and the ORR in the subgroups of patients who were aged <50 or <60 years compared with older patients. Although neither our study nor the previously published study (24) was powered to detect a statistical difference in these subgroups, the results could suggest that earlier administration of bevacizumab, or treatment with bevacizumab in younger patients, may lead to better tumor response and is something that requires investigation in further clinical trials.

Regarding the survival endpoints, our study showed results that were better than previously published data. The median OS of 10.5 months in GBM patients and 9.4 months in all patients was longer than that reported in other GBM trials (5.0–7.3 months) (6–8,10,11) and comparable with data with single-agent bevacizumab (9.3 months) (24,25). In addition, the 1-year survival rate for GBM patients (34.5%) was as good as the published data (14–32%) (6–8,10,11).

In addition to the favorable efficacy measures, a trend was also observed where 8 of the 11 patients who were taking corticosteroids at baseline were able to reduce their dose or discontinue corticosteroids altogether during the course of the study. This is consistent with other findings that suggest that bevacizumab may have corticosteroid-sparing effects in patients with recurrent GBM (39). Corticosteroid reduction may reduce infection rates and other related toxicities and therefore is expected to improve the health-related quality of life for patients.

Bevacizumab was well tolerated in our study and the incidence of AEs of special interest to bevacizumab was similar to that seen in other published studies with single-agent bevacizumab (24–26,40). No new bevacizumab safety signals were seen in this Japanese population.

In our study, and in the other single-agent bevacizumab studies (24–26,40), bevacizumab was administered after prior treatment with TMZ and RT. We observed an apparently greater benefit with bevacizumab in those patients with one relapse compared with those who have had two relapses following treatment with TMZ and RT. It is expected that bevacizumab may also provide benefit when administered concurrently with TMZ and RT rather than after TMZ/RT therapy. Currently, two randomized, double blind, Phase III studies are ongoing (AVAglio (41) and RTOG 0825 (42)) in which the addition of bevacizumab to standard of care (concurrent RT plus TMZ followed by adjuvant TMZ) is being evaluated in patients with newly diagnosed GBM.

There are many novel targeted agents under investigation for the treatment of gliomas (43); however, results with these new agents have been disappointing to date. Single-target agents alone may not be able to prevent tumor growth given the multiple pathways involved in many intracellular processes of tumor development. A key to future improvements in the treatment of gliomas will be the combination of other chemotherapeutic agents or molecular targeted therapies with bevacizumab to block these multiple pathways. This potential approach needs to be explored in future clinical trials.

In conclusion, the results of this study show that single-agent bevacizumab could provide significant clinical benefit for Japanese patients with recurrent GBM.

Acknowledgements

We are indebted to Dr Kazuhiro Nomura, Dr Shigeki Aoki and Tomoki Todo for their help in the assessment of efficacy and the evaluation of safety. We are also grateful to Dr Yoichi Nakazato for careful pathologic diagnosis.

Funding

This work was supported by Chugai Pharmaceutical Co. Ltd.

Conflict of interest statement

Dr Masao Matsutani is a coordinating investigator of this study, a member of the advisory committee on MSD KK and a member of the independent safety review board for Nobelpharma Co. Ltd; consulting fees as a coordinating investigator of this study have been received by him from Chugai Pharmaceutical Co. Ltd. Dr Ryo Nishikawa is a member of the Avaglio study steering committee (funded by F. Hoffmann-La Roche, Ltd) and has received research funding and speaking fees from MSD KK, and honoraria from Nobelpharma Co. Ltd. No other conflicts of interest were declared.

References

1. Hou LC, Veeravagu A, Hsu AR, Tse VC. Recurrent glioblastoma multiforme: a review of natural history and management options. *Neurosurg Focus* 2006;20:E5.
2. Ohgaki H. Epidemiology of brain tumors. *Methods Mol Biol* 2009;472:323–42.
3. Stupp R, Hegi ME, Mason WP, et al. Effects of radiotherapy with concomitant and adjuvant temozolomide versus radiotherapy alone on survival in glioblastoma in a randomised phase III study: 5-year analysis of the EORTC-NCIC trial. *Lancet Oncol* 2009;10: 459–66.
4. Stupp R, Mason WP, van den Bent MJ, et al. Radiotherapy plus concomitant and adjuvant temozolomide for glioblastoma. *N Engl J Med* 2005;352:987–96.
5. National Comprehensive Cancer Network. *NCCN Clinical Practice Guidelines in Oncology*. Central Nervous System Cancers V.2.2011. http://www.nccn.org/professionals/physician_gls/PDF/cns.pdf.
6. Lamborn KR, Yung WK, Chang SM, et al. Progression-free survival: an important end point in evaluating therapy for recurrent high-grade gliomas. *Neuro Oncol* 2008;10:162–70.
7. Ballman KV, Buckner JC, Brown PD, et al. The relationship between six-month progression-free survival and 12-month overall survival end points for phase II trials in patients with glioblastoma multiforme. *Neuro Oncol* 2007;9:29–38.
8. van den Bent MJ, Brandes AA, Rampling R, et al. Randomized phase II trial of erlotinib versus temozolomide or carmustine in recurrent glioblastoma: EORTC brain tumor group study 26034. *J Clin Oncol* 2009;27:1268–74.
9. Wong ET, Hess KR, Gleason MJ, et al. Outcomes and prognostic factors in recurrent glioma patients enrolled onto phase II clinical trials. *J Clin Oncol* 1999;17:2572–8.
10. Wick W, Puduvalli VK, Chamberlain MC, et al. Phase III study of enzastaurin compared with lomustine in the treatment of recurrent intracranial glioblastoma. *J Clin Oncol* 2010;28:1168–74.
11. Yung WK, Albright RE, Olson J, et al. A phase II study of temozolomide vs. procarbazine in patients with glioblastoma multiforme at first relapse. *Br J Cancer* 2000;83:588–93.
12. Huang H, Held-Feindt J, Buhl R, Mehdorn HM, Mentlein R. Expression of VEGF and its receptors in different brain tumors. *Neurol Res* 2005;27:371–7.
13. Chaudhry IH, O'Donovan DG, Brenchley PE, Reid H, Roberts IS. Vascular endothelial growth factor expression correlates with tumor grade and vascularity in gliomas. *Histopathology* 2001;39: 409–15.
14. Fukumura D, Xu L, Chen Y, Gohongi T, Seed B, Jain RK. Hypoxia and acidosis independently up-regulate vascular endothelial growth factor transcription in brain tumors *in vivo*. *Cancer Res* 2001;61: 6020–4.
15. Stefanik DF, Fellows WK, Rizkalla LR, et al. Monoclonal antibodies to vascular endothelial growth factor (VEGF) and the VEGF receptor, FLT-1, inhibit the growth of C6 glioma in a mouse xenograft. *J Neurooncol* 2001;55:91–100.
16. Hurwitz H, Fehrenbacher L, Novotny W, et al. Bevacizumab plus irinotecan, fluorouracil and leucovorin for metastatic colorectal cancer. *N Engl J Med* 2004;350:2335–42.
17. Johnson DH, Fehrenbacher L, Novotny W, et al. Randomised Phase II trial comparing bevacizumab plus carboplatin and paclitaxel with carboplatin and paclitaxel alone in previously untreated locally advanced or metastatic non-small-cell-lung cancer. *J Clin Oncol* 2004;22:2184–91.
18. Miller K, Wang M, Gralow J, et al. Paclitaxel plus bevacizumab versus paclitaxel alone for metastatic breast cancer. *N Engl J Med* 2007; 357:2666–76.
19. Yang JC, Haworth L, Sherry RM, et al. A randomised trial of bevacizumab, and anti-vascular endothelial growth factor antibody, for metastatic renal cancer. *N Engl J Med* 2003;349:427–34.
20. *How Avastin is Designed to Work [Internet]*. USA: Genentech, 2012 (cited 23 March 2012). http://www.avastin.com/avastin/patient/gbm/index.html.
21. *FDA Approves Drug for Treatment of Aggressive Brain Cancer [Internet]*. MD, USA: Food and Drug Administration, 2009 (cited 12 January 2012). www.fda.gov/NewsEvents/Newsroom/PressAnnouncements/2009/ucm152295.htm.
22. Stark-Vance V. Bevacizumab and CPT-11 in the treatment of relapsed malignant glioma. *Neuro-Oncol* 2005;7:369. Abstract 342.
23. Vrendenburgh JJ, Desjardins A, Herndon JE, II, et al. Bevacizumab plus irinotecan in recurrent glioblastoma multiforme. *J Clin Oncol* 2007;25:4722–9.
24. Friedman HS, Prados MD, Wen PY, et al. Bevacizumab alone and in combination with irinotecan in recurrent glioblastoma. *J Clin Oncol* 2009;27:4733–40.
25. Cloughesy T, Vredenburgh JJ, Day B, Das A, Friedman HS. Updated safety and survival of patients with relapsed glioblastoma treated with bevacizumab in the BRAIN study. *J Clin Oncol* 2010;28(Suppl):181s. Abstract 2008.
26. Kreisl TN, Kim L, Moore K, et al. Phase II trial of single-agent bevacizumab followed by bevacizumab plus irinotecan at tumor progression in recurrent glioblastoma. *J Clin Oncol* 2009; 27:740–5.
27. Raizer JJ, Grimm S, Chamberlain MC, et al. Phase 2 trial of single-agent bevacizumab given in an every-3-week schedule for patients with recurrent high-grade gliomas. *Cancer* 2010;116:5297–305.
28. Kairouz VF, Elias EF, Chahine GY, Comair YG, Dimassi H, Kamar FG. Final results of an extended phase II trial of bevacizumab and irinotecan in relapsed high grade gliomas. *Neuro-Oncol* 2010;12(Suppl 4):iv40–1. Abstract NO-20.
29. Gil MJ, de las Peñas R, Reynés G, et al. Bevacizumab plus irinotecan in recurrent malignant glioma showed high overall survival in a retrospective study. *Neuro-Oncol* 2010;12(Suppl. 4):iv53. Abstract NO-73.
30. Nghiemphu PL, Liu W, Lee Y, et al. Bevacizumab and chemotherapy for recurrent glioblastoma: a single-institution experience. *Neurology* 2009;72:1217–22.
31. Sathornsumetee S, Desjardins A, Vredenburgh JJ, et al. Phase II trial of bevacizumab and erlotinib in patients with recurrent malignant glioma. *Neuro-Oncol* 2010;12:1300–10.
32. Francesconi AB, Dupre S, Matos M, et al. Carboplatin and etoposide combined with bevacizumab for the treatment of recurrent glioblastoma multiforme. *J Clin Neurosci* 2010;17:970–4.
33. Soffietti R, Trevisan E, Ruda R, et al. Phase II trial of bevacizumab with fotemustine in recurrent glioblastoma: final results of a multicenter study of AINO (Italian Association of Neuro-oncology). *J Clin Oncol* 2011;29(Suppl):146. Abstract 2027.
34. Macdonald DR, Cascino TL, Schold SC, Cairncross JG. Response criteria for phase II studies of supratentorial malignant glioma. *J Clin Oncol* 1990;8:1277–80.
35. Trotti A, Colevas AD, Setser A, et al. CTCAE v3.0: development of a comprehensive grading system for the adverse effects of cancer treatment. *Semin Radiat Oncol* 2003;13:176–81.
36. Greenwood M. Reports on public health and medical subjects. The Error of Sampling of the Survivorship Tables. No 33, Appendix 1, London, UK: H.M Stationary Office, 1926.
37. Happold C, Roth P, Wick W, et al. ACNU-based chemotherapy for recurrent glioma in the temozolomide era. *J Neurooncol* 2009; 92:45–8.

38. Wen PY, Macdonald DR, Reardon DA, et al. Update response assessment criteria for high-grade gliomas: Response Assessment in Neuro-Oncology Working Group. *J Clin Oncol* 2010;28:1963–72.
39. Vredenburgh JJ, Cloughesy T, Samantc M, et al. Corticosteroid use in patients with glioblastoma at first or second relapse treated with bevacizumab in the BRAIN study. *Oncologist* 2010;15:1329–34.
40. Chamberlain MC, Johnston SK. Salvage therapy with single-agent bevacizumab for recurrent glioblastoma. *J Neurooncol* 2010;96:259–69.
41. *A Study of Avastin (bevacizumab) in Combination with Temozolomide and Radiotherapy in Patients with Newly Diagnosed Glioblastoma [Internet]*. USA: Clinicaltrials.gov, 2009 (cited 4 October 2011). http://clinicaltrials.gov/ct2/show/NCT00943826.
42. *Temozolomide and Radiation Therapy with or Without Bevacizumab in Treating Patients with Newly Diagnosed Glioblastoma [Internet]*. USA: Clinicaltrials.gov, 2009 (cited 4 October 2011). http://clinicaltrials.gov/ct2/show/NCT00884741.
43. Van Meir EG, Hadjipanayis CG, Norden AD, et al. Exciting new advances in neuro-oncology: the avenue to a cure for malignant glioma. *CA Cancer J Clin* 2010;60:166–93.

International Journal of
Radiation Oncology
biology • physics

www.redjournal.org

Clinical Investigation: Central Nervous System Tumor

Clinical Value of [^{11}C]Methionine PET for Stereotactic Radiation Therapy With Intensity Modulated Radiation Therapy to Metastatic Brain Tumors

Kazuhiro Miwa, MD,*,† Masayuki Matsuo, MD,§ Jun Shinoda, MD,*,† Tatsuki Aki, MD,*,† Shingo Yonezawa, MD,*,† Takeshi Ito, MD,‡ Yoshitaka Asano, MD,*,† Mikito Yamada, MD,‡ Kazutoshi Yokoyama, MD,‡ Jitsuhiro Yamada, MD,‡ Hirohito Yano, MD,‖ and Toru Iwama, MD‖

**Chubu Medical Center for Prolonged Traumatic Brain Dysfunction, Kizawa Memorial Hospital, Minokamo, Gifu, Japan; †Department of Clinical Brain Sciences, Gifu University Graduate School of Medicine, Minokamo, Gifu, Japan; ‡Department of Neurosurgery, Kizawa Memorial Hospital, Minokamo, Gifu, Japan; §Department of Radiation Oncology, Kizawa Memorial Hospital, Minokamo, Gifu, Japan; and ‖Department of Neurosurgery, Gifu University Graduate School of Medicine, Gifu, Japan*

Received May 16, 2011, and in revised form Feb 15, 2012. Accepted for publication Feb 16, 2012

Summary

We investigated the impact of [^{11}C]methionine-positron emission tomography (MET-PET) for SRT-IMRT in brain metastasis. In 42 tumors, gross tumor volume was defined by magnetic resonance imaging (MRI) with MET-PET. MET uptake values in tumors before and after SRT-IMRT were evaluated and compared with MRI examination. Consequently, the differences in MET uptake between the pre-SRT-IMRT group and post-SRT-IMRT group were statistically significant, irrespective of MRI

Purpose: This study investigated the clinical impact of ^{11}C-labeled methionine-positron emission tomography (MET-PET) for stereotactic radiation therapy with intensity modulated radiation therapy (SRT-IMRT) in metastatic brain tumors.

Methods and Materials: Forty-two metastatic brain tumors were examined. All tumors were treated with SRT-IMRT using a helical tomotherapy system. Gross tumor volume (GTV) was defined and drawn on the stereotactic magnetic resonance (MR) image, taking into account the respective contributions of MR imaging and MET-PET. Planning target volume (PTV) encompassed the GTV-PET plus a 2-mm margin. SRT-IMRT was performed, keeping the dose for PTV at 25-35 Gy in 5 fractions. The ratio of the mean value of MET uptake to the contralateral normal brain (L/N ratio) was plotted for the PTV prior to SRT-IMRT, at 3 months following SRT-IMRT, and at 6 months following SRT-IMRT. Tumor characteristic changes of MET uptake before and after SRT-IMRT were evaluated quantitatively, comparing them with MRI examination.

Results: Mean ± SD L/N ratios were 1.95 ± 0.83, 1.18 ± 0.21, and 1.12 ± 0.25 in the pre-SRT-IMRT group, in the 3 months post-SRT-IMRT group, and in the 6 months post-SRT-IMRT group, respectively. Differences in the mean L/N ratio between the pre-SRT-IMRT group and the 3-month post-SRT-IMRT group and between the pre-SRT-IMRT group and the 6 month post-SRT-IMRT group were statistically significant, irrespective of MRI examination.

Conclusions: We showed examples of metastatic lesions demonstrating significant decreases in MET uptake following SRT-IMRT. MET-PET seems to have a potential role in providing additional information, although MRI remains the gold standard for diagnosis and follow-up after SRT-IMRT. The present study is a preliminary approach, but to more clearly define the impact

Reprint requests to: Kazuhiro Miwa, MD, Department of Neurosurgery, Chubu Medical Center for Prolonged Traumatic Brain Dysfunction, Kizawa Memorial Hospital, 630 Shimokobi, Kobi-cho, Minokamo, Gifu 505-0034, Japan. Tel: +81-574-24-2233; Fax: +81-574-24-2230; E-mail: doctor.3@jasmine.ocn.ne.jp

Conflict of interest: none.

Int J Radiation Oncol Biol Phys, Vol. 84, No. 5, pp. 1139–1144, 2012
0360-3016/$ - see front matter
doi:10.1016/j.ijrobp.2012.02.032

examination. MET-PET may have a potential role in providing additional information for the diagnosis and follow-up after SRT-IMRT.

of PET-based radiosurgical assessment, further experimental and clinical analyses are required.

Introduction

The higher specificity and sensitivity of ^{11}C-labeled methionine-positron emission tomography (MET-PET) in imaging of brain tumors has been demonstrated in previous studies and may be helpful for detection of the tumor and for assessment of radiosurgical treatment (1-3). Recently, a technique has been developed that allows routine integration of PET in stereotactic radiosurgery (4-7).

This study investigated the clinical impact of MET-PET for stereotactic radiation therapy with intensity modulated radiation therapy (SRT-IMRT) in brain metastases. In this preliminary study, MET-PET images were imported into the planning software for SRT-IMRT dosimetry, and the final target volume was defined and drawn on the stereotactic magnetic resonance (MR) image. Finally, we investigated the characteristic changes of MET-PET in tumors for monitoring after SRT-IMRT and evaluated differences between the image changes on MET-PET compared to those on MRI.

Methods and Materials

Patient population

Twenty patients with a total of 42 metastatic brain tumors were treated with SRT-IMRT at Kizawa Memorial Hospital between February 2008 and May 2010. Patients and metastases characteristics are shown in Tables 1 and 2. Computed tomography, MRI, and MET-PET were performed separately within 1 week in all 20 patients for SRT-IMRT treatment planning. Eight patients had multiple metastatic brain tumors. Karnofsky performance status levels were between 70% and 100% (mean, 80%). Our institutional ethics committee approved the study protocol, and all patients provided written informed consent.

PET methods

The PET scanner was an Advance NXi Imaging System (General Electric Yokokawa Medical System, Hino-shi, Tokyo), which provides 35 transaxial images at 4.25-mm intervals. The in-plane spatial resolution (full width at half-maximum) was 4.8 mm, and scans were performed in standard 2-dimensional mode. Before emission scans were performed, a 3-min transmission scan was performed to correct photon attenuation,using a ring source containing ^{68}Ge. A dose of 7.0 MBq/kg MET was injected intravenously into the cubital vein within 1 min. Emission scans were acquired for 30-min, beginning 5 min after MET injection. During MET-PET data acquisition, head motion was continuously monitored using laser beams projected onto ink markers drawn over the forehead skin and was corrected as necessary.

MRI methods

MRI for radiation treatment planning was performed using 1.5-T equipment (Signa Horizon LX; General Electric, Waukesha, WI). Acquisitions were made using a standard head coil without rigid immobilization. An axial, 3D gradient echo T1-weighted sequence with contrast medium (0.1 mmol/kg body weight, gadolinium-diethylenetriamine-pentaacetic acid [Gd-DTPA]; Magnevist, Schering, Berlin, Germany), and 2.0-mm slice thicknesses were acquired from the foramen magnum to the vertex, perpendicular to the main magnetic field.

Treatment protocol

Image registrations were performed using Syntegra software (Philips Medical System), using a combination of automatic and manual methods. Quantitative accuracy of the mutual information registration was evaluated and approved by 3 observers, (ie, a neurosurgeon, a radiation oncologist, and a nuclear medicine specialist). The 3 observers delineated gross target volume (GTV) by using MRI. Planning began with a separate analysis of each stereotactic imaging modality. A 3D volumetric contour was drawn on stereotactic MR images, corresponding to the area of Gd-DTPA enhancement. Then, the stereotactic PET images are analyzed independently by the 3 observers together. Abnormal PET signal suitable for target definition corresponded to areas of increased tracer uptake compared with the surrounding normal brain. A 3D volumetric PET contour delineating these areas was drawn on a visual basis and projected onto the corresponding MR images. Finally, GTV was defined and drawn on the stereotactic MR image, taking into account the respective contributions of MET-PET and MRI, as well as the anatomic location of the tumor and the functional areas at risk (Fig. 1). The planning target volume (PTV) of SRT-IMRT encompassed the GTV plus a 2-mm

Table 1 Patient characteristics

Characteristic	No. of patients (% or range)
No. of patients	20
Gender	
Male	9 (45)
Female	11 (55)
Age	
Mean (range)	61.3 (42-84 y)
Diagnosis	
NSCLC	10 (50)
Breast cancer	6 (30)
Colon cancer	2 (10)
Renal cell cancer	1 (5)
Other	1 (5)

Abbreviation: NSCLC = non-small cell lung cancer.

Table 2 Metastases characteristics

Characteristic	No. of patients (n=42%)
Gender	
Male	12 (29)
Female	30 (71)
Diagnosis	
NSCLC	23 (55)
Breast cancer	15 (36)
Colon cancer	2 (5)
Renal cell cancer	1 (2)
Other	1 (2)

Abbreviation: NSCLC = non-small cell lung cancer.

margin. SRT-IMRT was performed using HT (helical TomoTherapy; TomoTherapy Inc) in 5 fractions, keeping the dose for PTV at 25 Gy in 10 lesions, 30 Gy in 17 lesions, and 35 Gy in 15 lesions. This dose was prescribed using the 95% isodose line, which covered the PTV.

Follow-up study

For the follow-up study, each patient underwent a series of MET-PET and MRI examinations consisting of a baseline examination prior to SRT-IMRT, at 3 months after SRT-IMRT, and at 6 months following SRT-IMRT. Patients who died after SRT-IMRT were excluded from follow-up at that point. In each case, characteristic changes of MET uptake in lesions post-SRT-IMRT were evaluated quantitatively.

Quantitative evaluation consisted of measurement of the MET uptake value at the PTV. As a normal control, several circular regions of interests with a diameter of 10 mm were located over the gray matter of the contralateral frontal lobe. The lesion vs normal (L/N) ratio was defined as the mean counts of radioisotope per pixel in the lesion of the PTV divided by the mean counts per pixel in the contralateral normal frontal lobe. The L/N ratio within the PTV was calculated prior to SRT-IMRT, at 3 months after SRT-IMRT, and at 6 months after SRT-IMRT. Differences between the 3 groups were examined statistically (see Statistical analysis below).

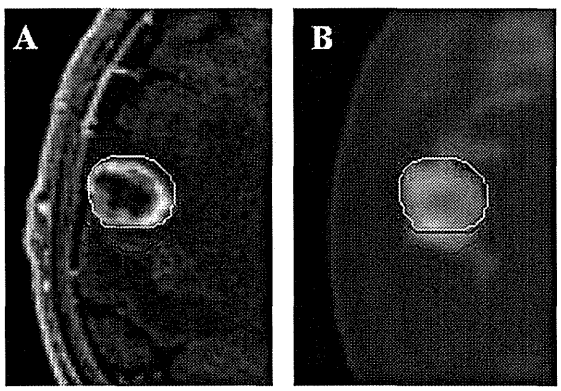

Fig. 1. Dose map of a representative case with MRI (A) and [^{11}C]MET-PET (B). In this case, the lesion's abnormal MET uptake (yellow line) extended beyond the gadolinium-enhanced lesion on MRI (red line). We defined GTV including the lesion of abnormal MET uptake, and the PTV encompassed the GTV-PET plus a 2-mm margin.

On MRI, the tumor responses of SRT-IMRT were classified into 3 types: complete response or partial response (type A), no change (type B), or progressive disease (type C), all determined by the changes in the volume of Gd-DTPA enhancement at 3 months after SRT-IMRT. In each type classified by MRI examination, the L/N ratio of the MET uptake within the PTV was calculated prior to SRT-IMRT, at 3 months after SRT-IMRT, and at 6 months after SRT-IMRT.

A definitive diagnosis of recurrent tumor or radiation necrosis was determined as follows. Recurrence was defined as a case in which pathologic diagnosis was confirmed by tumor resection or biopsy. Diagnosis of radiation necrosis was based on pathologic examination or clinical course. Cases in which lesions showed spontaneous shrinkage or remained stable in size on MRI after a long-term follow-up were assumed to be a delayed tumor response, which could represent radiation necrosis.

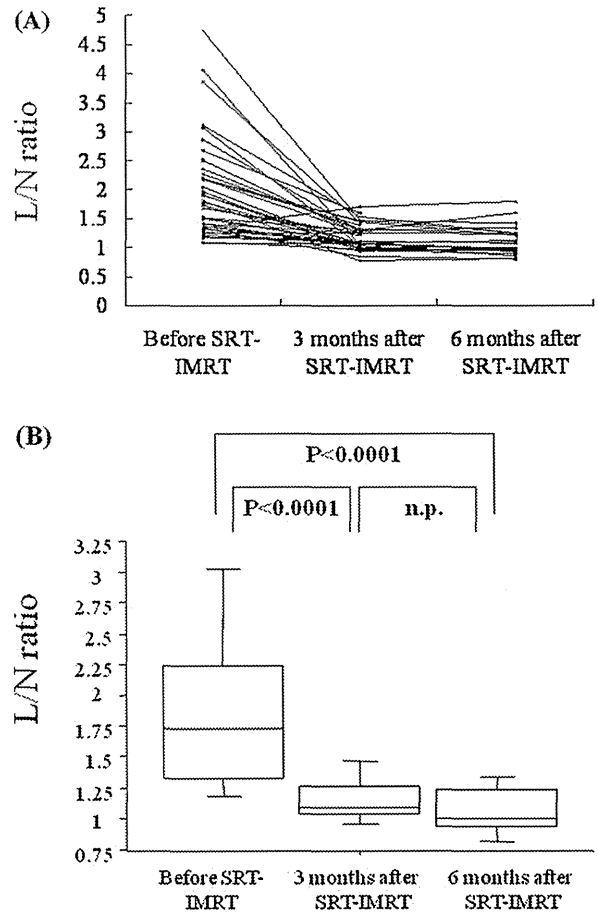

Fig. 2. (A) The ratio of the mean value of [^{11}C]MET uptake to the contralateral normal brain (L/N ratio) plotted at the PTV prior to SRT-IMRT, at 3 months after SRT-IMRT, and at 6 months after SRT-IMRT. (B) Boxplots divide data into 4 qualities. Lower and upper borders of the box represent the 25th and the 75th percentiles, respectively; the middle line represents the median value. The difference in the L/N ratio between the pre-SRT-IMRT group and the 3-month post-SRT-IMRT group was significant ($P<.0001$), as was the difference between the pre-SRT-IMRT group and the 6-month post-SRT-IMRT group ($P<.0001$).

Statistical analysis

All data were analyzed using a commercial statistical software package (StatView, version 5.0J; SAS Institute, Cary, NC). Statistical analysis was performed to compare the L/N ratios among 3 groups (prior to SRT, at 3 months after SRT, and at 6 months after SRT) by using nonparametric Friedman's test. For all statistics, a probability value less than .05 was considered significant. All data are expressed asmeans ± SD.

Results

Follow-up studies were performed in all 42 tumors at 3 months after SRT-IMRT and in 24 tumors at 6 months after SRT-IMRT. Eighteen tumors of 8 patients were lost to follow-up 6 months after SRT-IMRT because those patientsdied from systemic disease within 6 months after SRT-IMRT.

In 23 of a total of 42 tumors, MRI with PET-based GTV was larger than MRI-based GTV. The average GTV defined by MRI alone was 8.01 ± 11.83 cm^3, and the average GTV defined by MRI with PET was 8.94 ± 12.29 cm^3. The average GTV increased by 10.4% when MRI with PET was used vs when MRI alone was used.

Results of the follow-up studies of quantitative analyses in all tumors are shown in Figure 2. L/N ratios were 1.95 ± 0.83, 1.18 ± 0.21, and 1.12 ± 0.25 in the pre-SRT-IMRT group, in the 3 month post-SRT-IMRT group, and in the 6 month post-SRT-IMRT group, respectively. Differences in the L/N ratios between the pre-SRT-IMRT group and the 3-month post-SRT-IMRT group was significant ($P<.0001$) and that between the pre-SRT-IMRT group and the 6-month post-SRT-IMRT group was also significant ($P<.0001$).

Results of analyses in each type classified by the volume change of Gd-DTPA enhancement are shown in Figure 3A, B, and C. The number of tumors in each type was 28, 7, and 7, respectively. In type A, the L/N ratios were 1.93 ± 0.98, 1.14 ± 0.19, and 1.05 ± 0.14 in the pre-SRT-IMRT, the 3-month post-SRT-IMRT group, and the 6-month post-SRT-IMRT group. In type B, the L/N ratios were 1.96 ± 0.28, 1.17 ± 0.26, and 1.11 ± 0.29 in the pre-SRT-IMRT group, the 3-month post-SRT-IMRT group, and the 6-month post-SRT-IMRT group. In type C, the L/N ratios were 2.04 ± 0.59, 1.31 ± 0.23, and 1.30 ± 0.35 in the pre-SRT-IMRT group, the 3-month post-SRT-IMRT group, and the 6-month post-SRT-IMRT group. In each of the 3 types, the differences in the L/N ratios between the pre-SRT-IMRT group and the 3-month post-SRT-IMRT group were significant ($P=.0001$ in type A; $P=.0003$ in type B; and $P=.0172$ in type C), and those between the pre-SRT-IMRT group and the 6-month post-SRT-IMRT group were also significant ($P=.0005$ in type A; $P=.0002$ in type B; and $P=.0294$ in type C).

Local recurrence was defined in two of a total of 42 tumors after SRT-IMRT. No recurrence was demonstrated in all tumors of type A. In one tumor of type B, the L/N ratio was decreased from 1.52-1.30 at 3 months after SRT-IMRT, but it was increased to

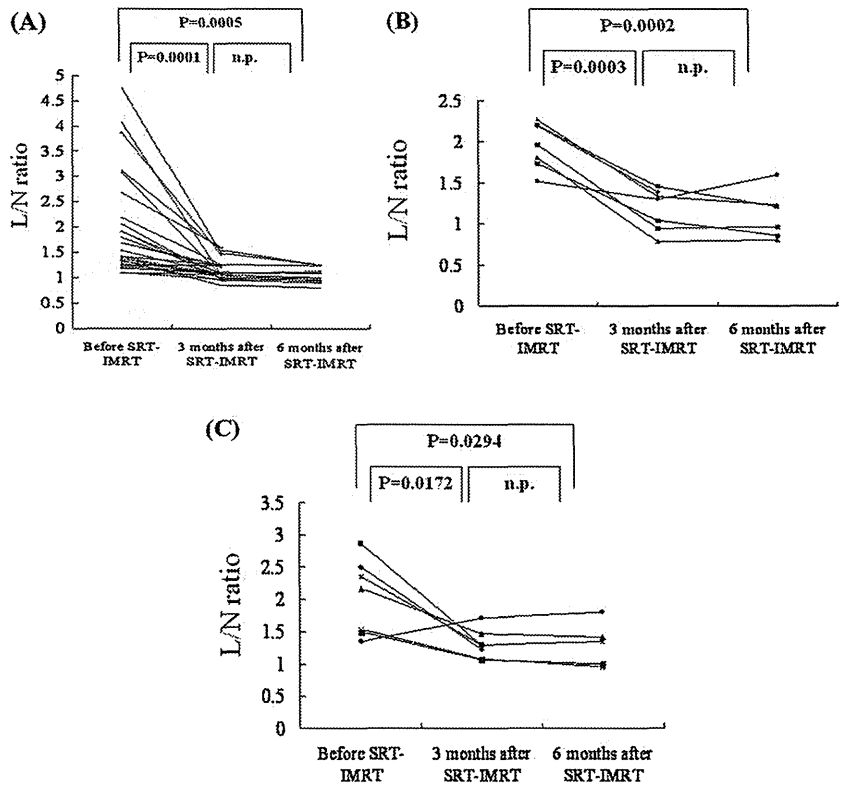

Fig. 3. The L/N ratio plotted at the PTV prior to SRT-IMRT, at 3 months after SRT-IMRT, and at 6 months after SRT-IMRT in each type classified by MRI examination. Complete response or partial response (A), no change (B), or progressive disease (C), all determined by the changes in the volume of contrast enhancement 3 months after SRT-IMRT. The number of tumors in each type was 28, 7, and 7, respectively. In each of the 3 types, differences in the L/N ratios between the pre-SRT-IMRT group and the 3-month post-SRT-IMRT group was significant ($P=.0001$ in type A; $P=.0003$ in type B; and $P=.0172$ in type C) and that between the pre-SRT-IMRT group and the 6-month post-SRT-IMRT group was also significant ($P=.0005$ in type A; $P=.0002$ in type B; and $P=.0294$ in type C).

1.60 in the next 3 months, and marginal tumor recurrence was defined at 9 months after SRT-IMRT. In one tumor of type C, the L/N ratio was increased from 1.34-1.71 at 3 months after SRT-IMRT, and marginal tumor recurrence was defined at 6 months after SRT-IMRT. In the other 6 tumors of type C, the L/N ratio was decreased after SRT-IMRT, and lesions showed spontaneous shrinkage or remained stable in size after a long-term follow-up, which were assumed to be radiation necrosis. Follow-up terms of these 6 tumors ranged from 19-43 months. A representative case of type C is shown in Figure 4. In the acute and subacute phases, there was no neurologic toxicity from SRT-IMRT in all cases.

Discussion

The use of PET, an imaging technique providing metabolic data, may play an important role in improving the radiosurgical treatment of malignant brain tumors (1-3, 8-10). In recent PET studies, analysis of the metabolic and histological characteristics of a stereotactic biopsy specimen provided evidence that regional high MET uptake correlated with the presence of viable tumor cells (11). Baumert et al (12) demonstrated the data correlated MRI findings with histology, in which an infiltrative growth beyond the border of the brain metastasis in 63% cases evaluated. Along the same line, the relationship between pathology and metabolism found in stereotactic biopsy and the increased knowledge about MET-PET in brain tumor strengthen the valuable link between MET uptake and histology. Matsuo et al (13) demonstrated that there was severe discrepancy between PET- and MRI-defined target volumes in their report of metastatic brain tumors, and those findings suggested that MET-PET might significantly improve the definition of target volumes in patients with brain metastases (13).

Based on those recent PET studies, MET-PET images were imported in the planning software for the SRT-IMRT dosimetry as the supplemental information in this preliminary study, and the final target volume was defined and drawn on the stereotactic MR image, taking into account the respective contributions of MET-PET and MRI (Fig. 1). In this report, we describe our preliminary experience with the complementary use of PET metabolic data in an HT system, which uses a patented multileaf collimator to modulate the intensity of the beam, precisely conforming to the shape of the tumor, so it can deliver IMRT technique (14-18). There was no acute or subacute neurologic toxicity from SRT-IMRT in all our cases.

Data from this study demonstrated the utility of MET-PET imaging in monitoring the characteristic changes following SRT-IMRT. By quantitative statistical evaluation, the differences in L/N ratios between the pre-SRT-IMRT group and 3-month post-SRT-IMRT group was significant ($P<.0001$) and that between the pre-SRT-IMRT group and 6-month post-SRT-IMRT group was also significant ($P<.0001$) (Fig. 2). It would seem that those significant decreases of MET uptake could be secondary to metabolic changes

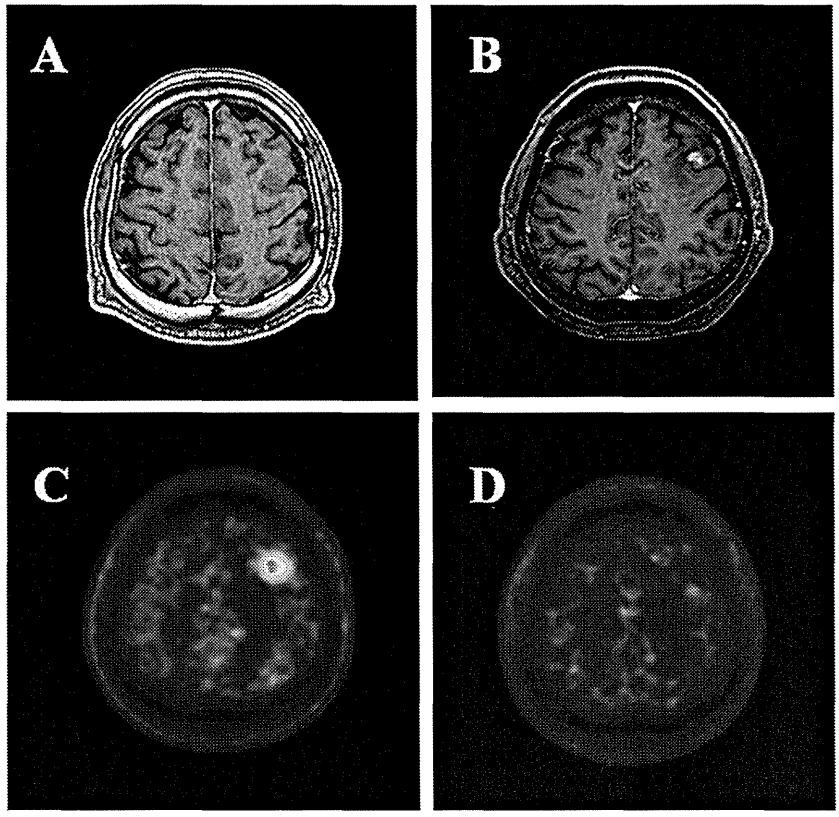

Fig. 4. A 53-year-old male patient with non-small cell lung cancer. Gadolinium-enhanced MRI before SRT-IMRT (A) and 3 months after SRT-IMRT (B), and MET-PET before SRT-IMRT (C) and 3 months after SRT-IMRT (D). Metastatic brain tumor in the left frontal lobe is demonstrated, showing no Gd-enhancement at all on MRI but high MET uptake on PET (A and C). At 3 months after SRT-IMRT, the volume of Gd-enhanced lesion on MRI increased, although MET uptake at the lesion distinctly decreased (B and D). The lesion remained stable in size on MRI after a long-term follow-up, which was assumed to be radiation necrosis.

of target lesion, which suspected the intensive radiosurgical efficacy to the metabolic condition in tumors. The result suggested that reduced MET uptake following SRT-IMRT should be attributed to deactivation and/or obliteration of viable cancer cells after radiation treatment, although other explanations, such as changes in the vasculature or edema/inflammation, must also be considered for the reason of reduced MET uptake. From the follow-up study, marginal tumor recurrence was defined in 2 of 42 tumors, with increasing MET uptake after SRT-IMRT. Local tumor control by SRT-IMRT seemed to be favorable from the results of the follow-up study, so that contouring of the GTV by respective contributions of MET-PET and MRI were thought to be acceptable. Eighteen tumors were lost to follow-up at 6 months after SRT-IMRT. However, we believe that selection bias could be avoided because the reason patients were lost to follow-up was not from neurological death by the metastatic brain tumor.

The present analysis demonstrates that MET-PET containing metabolic information is independent of the morphologic information provided by MRI. The significant difference of MET uptake had been demonstrated in the L/N ratio between the pre-SRT-IMRT group and the post-SRT-IMRT group, irrespective of the type of MRI examination (Fig. 3). In 6 tumors of type C with decreasing MET uptake lesions showed spontaneous shrinkage or remained stable in size on MRI after a long-term follow-up, which was suspicious for radiation injury rather than tumor recurrence (Fig. 4). In the previous report, early delayed reactions occurred from a few weeks to several months later than the subacute reactions following conventional fractionated radiation therapy or radiosurgery (19). This was probably due to temporary demyelination and vascular damage and may prove fully or partially reversible. Tumor swelling sometimes occurs in the early delayed phase and is associated with edema in the surrounding normal brain. Tumor shrinkage occurs later, with subsidence of the surrounding edema. Similarly, contrast enhancement at this time, particularly in the tumor perimeter, reflects a host of reactive responses and not tumor activity. Sometimes it is not easy to distinguish this phenomenon from tumor recurrence with conventional Gd-DTPA-enhanced MR examinations (20).

In the follow-up study after RT, the value of MET-PET was reported to be a sensitive and accurate technique for differentiating between tumor recurrence and radiation injury following stereotactic radiosurgery (9). The current study demonstrates the dynamic change of metabolic condition with MET-PET studies before and after SRT-IMRT, which seems to be appropriate for the differential diagnosis of tumor recurrence from radiation injury. Especially in cases with increasing volume on MRI after SRT-IMRT, results of the dynamic change of MET-PET studies might be helpful for clinical diagnoses. We considered the fact that because MRI has high sensitivity but poor specificity, it should be used first as a screening test. In the event of suspected tumor recurrence, additional MET-PET investigation seems to differentiate between post-treatment changes and tumor recurrence and to avoid both under- and overtreatment, although further studies are needed.

Conclusions

In conclusion, MET-PET seems to have a potential role in providing additional information for treatment by SRT-IMRT, although MRI remains the gold standard for the diagnosis and follow-up of metastatic brain tumors. The present study is a preliminary approach, and the sample size of the study seems to be small for this evaluation, but to more clearly define the impact of PET-based SRT-IMRT planning and monitoring, further experimental and clinical analyses are required.

References

1. Chen W. Clinical applications of PET in brain tumors. *J Nucl Med* 2007;48:1468-1481.
2. Herholz K, Coope D, Jackson A. Metabolic and molecular imaging in neuro-oncology. *Lancet Neurol* 2007;6:711-724.
3. Evans ES, Hahn CA, Kocak Z, et al. The role of functional imaging in the diagnosis and management of late normal tissue injury. *Semin Radiat Oncol* 2007;17:72-80.
4. Levivier M, Massager N, Wikler D, et al. Use of stereotactic PET images in dosimetry planning of radiosurgery for brain tumors: clinical experience and proposed classification. *J Nucl Med* 2004;45: 1146-1154.
5. Grosu AL, Lachner R, Wiedenmann N, et al. Validation of a method for automatic image fusion (BrainLAB System) of computed tomography data and 11C-methionine-PET data for stereotactic radiotherapy using a LINAC: first clinical experience. *Int J Radiat Oncol Biol Phys* 2003;56:1450-1463.
6. Levivier M, Wikier D, Goldman S, et al. Integration of the metabolic data of positron emission tomography in the dosimetry planning of radiosurgery with the gamma knife: early experience with brain tumors. Technical note. *J Neurosurg* 2000;93(suppl):S233-S238.
7. Levivier M, Massager N, Wikler D, et al. Integration of functional imaging in radiosurgery: the example of PET scan. *Prog Neurol Surg* 2007;20:68-81.
8. Jacobs AH, Kracht LW, Gossmann A, et al. Imaging in neurooncology. *NeuroRx* 2005;2:333-347.
9. Tsuyuguchi N, Sunada I, Iwai Y, et al. Methionine positron emission tomography of recurrent metastatic brain tumor and radiation necrosis after stereotactic radiosurgery: is a differential diagnosis possible? *J Neurosurg* 2003;98:1056-1064.
10. Ross DA, Sandler HM, Balter JM, et al. Imaging changes after stereotactic radiosurgery of primary and secondary malignant brain tumors. *J Neurooncol* 2002;56:175-181.
11. Pirotte B, Goldman S, Massager N, et al. Combined use of 18F-fluorodeoxyglucose and 11C-methionine in 45 positron emission tomography-guided stereotactic brain biopsies. *J Neurosurg* 2004;101: 476-483.
12. Baumert BG, Rutten I, Dehing-Oberije C, et al. A pathology-based substrate for target definition in radiosurgery of brain metastases. *Int J Radiat Oncol Biol Phys* 2006;66:187-194.
13. Matsuo M, Miwa K, Shinoda J, et al. Target definition by C11-methionine-PET for the radiotherapy of brain metastases. *Int J Radiat Oncol Biol Phys* 2009;74:714-722.
14. Baisden JM, Benedict SH, Sheng K, et al. Helical TomoTherapy in the treatment of central nervous system metastasis. *Neurosurg Focus* 2007;22:E8.
15. Bauman G, Yartsev S, Fisher B, et al. Simultaneous infield boost with helical tomotherapy for patients with 1-3 brain metastases. *Am J Clin Oncol* 2007;30:38-44.
16. Bauman G, Yartsev S, Rodrigues G, et al. A prospective evaluation of helical tomotherapy. *Int J Radiat Oncol Biol Phys* 2007;68:632-641.
17. Yartsev S, Kron T, Cozzi L, et al. Tomotherapy planning of small brain tumours. *Radiother Oncol* 2005;74:49-52.
18. Welsh JS, Patel RR, Ritter MA, et al. Helical tomotherapy: an innovative technology and approach to radiation therapy. *Technol Cancer Res Treat* 2002;1:311-316.
19. Plowman PN. Stereotactic radiosurgery. VIII. The classification of postradiation reactions. *Br J Neurosurg* 1999;13:256-264.
20. Nishimura R, Takahashi M, Morishita S, et al. MR Gd-DTPA enhancement of radiation brain injury. *Radiat Med* 1992;10:109-116.

ELSEVIER

Int. J. Radiation Oncology Biol. Phys., Vol. 82, No. 1, pp. 83–89, 2012

0360-3016/$ - see front matter

doi:10.1016/j.ijrobp.2010.09.020

CLINICAL INVESTIGATION **Central Nervous System Tumor**

IMPACT OF [^{11}C]METHIONINE POSITRON EMISSION TOMOGRAPHY FOR TARGET DEFINITION OF GLIOBLASTOMA MULTIFORME IN RADIATION THERAPY PLANNING

MASAYUKI MATSUO, M.D.,* KAZUHIRO MIWA, M.D.,† OSAMU TANAKA, M.D.,* JUN SHINODA, M.D.,† HIRONORI NISHIBORI, M.D.,‡ YUSUKE TSUGE, M.D.,‡ HIROHITO YANO, M.D.,¶ TORU IWAMA, M.D.,¶ SHINYA HAYASHI, M.D.,§ HIROAKI HOSHI, M.D.,§ JITSUHIRO YAMADA, M.D.,† MASAYUKI KANEMATSU, M.D.,§ AND HIDEFUMI AOYAMA, M.D.**

*Department of Radiation Oncology, Kizawa Memorial Hospital, Minokamo, Japan; †Chubu Medical Center for Prolonged Traumatic Brain Dysfunction and Department of Clinical Brain Sciences, Gifu University Graduate School of Medicine, Minokamo, Japan; ‡Department of Radiology, Kizawa Memorial Hospital, Minokamo, Japan; Departments of ¶Neurosurgery and §Radiology, Gifu University School of Medicine, Gifu, Japan; **Department of Radiology, Niigata University School of Medicine, Niigata, Japan

Purpose: The purpose of this work was to define the optimal margins for gadolinium-enhanced T_1-weighted magnetic resonance imaging (Gd-MRI) and T_2-weighted MRI (T_2-MRI) for delineating target volumes in planning radiation therapy for postoperative patients with newly diagnosed glioblastoma multiforme (GBM) by comparison to carbon-11-labeled methionine positron emission tomography ([^{11}C]MET-PET) findings.

Methods and Materials: Computed tomography (CT), MRI, and [^{11}C]MET-PET were separately performed for radiation therapy planning for 32 patients newly diagnosed with GBM within 2 weeks after undergoing surgery. The extent of Gd-MRI (Gd-enhanced clinical target volume [CTV-Gd]) uptake and that of T_2-MRI of the CTV (CTV-T_2) were compared with the extent of [^{11}C]MET-PET (CTV–[^{11}C]MET-PET) uptake by using CT–MRI or CT–[^{11}C]MET-PET fusion imaging. We defined CTV-Gd (x mm) and CTV-T_2 (x mm) as the x-mm margins (where x = 0, 2, 5, 10, and 20 mm) outside the CTV-Gd and the CTV-T_2, respectively. We evaluated the relationship between CTV-Gd (x mm) and CTV– [^{11}C]MET-PET and the relationship between CTV-T_2 (x mm) and CTV– [^{11}C] MET-PET.

Results: The sensitivity of CTV-Gd (20 mm) (86.4%) was significantly higher than that of the other CTV-Gd. The sensitivity of CTV-T_2 (20 mm) (96.4%) was significantly higher than that of the other CTV-T_2 (x = 0, 2, 5, 10 mm). The highest sensitivity and lowest specificity was found with CTV-T_2 (x = 20 mm).

Conclusions: It is necessary to use a margin of at least 2 cm for CTV-T_2 for the initial target planning of radiation therapy. However, there is a limit to this setting in defining the optimal margin for Gd-MRI and T_2-MRI for the precise delineation of target volumes in radiation therapy planning for postoperative patients with GBM.

[^{11}C]Methionine-PET, Glioblastoma, Radiotherapy, Target definition, MRI.

INTRODUCTION

Glioblastoma multiforme (GBM) is the most common type of primary brain tumor in adults, and the treatment of GBM remains one of the most challenging endeavors in oncologic treatment. The current standard of care for newly diagnosed GBM is surgical resection, to the extent that it is feasible, followed by adjuvant radiotherapy and chemotherapy (1). Several studies over the past few decades have attempted to define the optimal radiation dose for GBM, yet the results have not been satisfying (2–4).

Highly accurate radiation therapy techniques such as stereotactic radiotherapy, radiosurgery, intensity-modulated radiotherapy, and proton therapy have recently developed. Improved survival by using such highly accurate radiation therapy is possible because high-dose irradiation to a limited target volume eradicates tumor cells while minimizing radiation exposure to normal, functional brain tissue. For this therapy to succeed, the first premise is that the extent of tumor must be correctly defined. Accurate definitions of the gross target volume (GTV) and the clinical target volume (CTV) are crucial.

To determine the radiation therapy treatment volume for GBM, many studies have used the enhanced area or peritumoral edema area on magnetic resonance imaging (MRI)

Reprint requests to: Masayuki Matsuo, M.D., Department of Radiation Oncology, Kizawa Memorial Hospital, 590 Shimokobi, Minokamo 505-8503, Japan. Tel: (+81) 574-26-2181; Fax: (+81) 574-25-2181; E-mail: matsuo@kizawa-memorial-hospital.jp

Conflict of interest: none.

Received June 9, 2010, and accepted for publication Sept 28, 2010.

or computed tomography (CT), respectively, to determine initial radiation treatment volume as well as boost volume (5–7). For instance, the method for target delineation of GBM at the University of Texas M. D. Anderson Cancer Center has been to define the CTV as the enhanced area (GTV) plus 2 cm and the planning target volume (PTV) as the CTV plus 0.5 cm (5). An alternate method, used by the Radiation Therapy Oncology Group (RTOG), is to define the initial field as the peritumoral edema plus 2 cm and the dose prescribed to this area is 46 Gy. The boost field is defined as the GTV plus 2.5 cm, and the dose prescribe to this area is 60 Gy (5–7). However, evidence for the margin of the enhanced area or the peritumoral edema of the GBM tumor is not sufficient (5).

Positron emission tomography (PET) has been used for 2 decades to assess the cerebral metabolism of patients with gliomas (8, 9). Carbon-11-labeled methionine PET ([^{11}C]MET-PET) plays an especially important role in improving diagnostic procedures for treating brain tumors (10). [^{11}C]Methionine is not taken up by normal brain tissue to a marked degree, and the sensitivity of [^{11}C]MET-PET for detecting glioma tumors appears to be high (11–16). [^{11}C]MET-PET uptake by normal brain parenchyma is relatively low, and so [^{11}C]MET-PET shows promise for assessing cerebral tumor dimensions (17). It has been suggested that [^{11}C]MET-PET may more precisely outline the true extent of viable tumor tissue than MRI, whereas MRI has the capability to better delineate the total extent of associated pathologic changes, such as edema, in adjacent brain areas (18).

We undertook the present study of quantified results of [^{11}C]MET-PET and those of MRI to compare their abilities to delineate the extent of GBM and to show the implications of [^{11}C]MET-PET for treatment planning. Therefore, the extent of gadolinium (Gd) enhancement on T_1-weighted MRI and the high-intensity area on T_2-weighted MRI were compared with the extent of uptake of [^{11}C]MET-PET by using CT–MRI or CT–[^{11}C]MET-PET fusion imaging. We conducted this study to investigate the extent to which tumor growth was present and to quantify this growth in GBM by comparing MRI and [^{11}C]MET-PET. We assumed [^{11}C]MET-PET was the gold standard in this study for delineating the CTV, and we determined the optimal margins of Gd enhancement and high-intensity areas on T_2-weighted imaging. We evaluated the validity of the margins by comparison with those reported in a study by Jansen et al. (19), which correlated results of histopathologic observations with CT/MR images.

METHODS AND MATERIALS

During the 2-year period between April 2006 and December 2008, 32 postoperative patients, newly diagnosed and histologically confirmed with GBM (Table 1), underwent stereotactic radiotherapy treatment planning at our department.

CT, Gd-enhanced T_1-weighted and T_2-weighted MRI, and [^{11}C]MET-PET were performed separately within 2 weeks after the 32 patients (18 men and 14 women; age range, 21-85 years; mean age, 64 years) underwent surgery. Steroid doses were not changed during the week in which MRI and [^{11}C]MET-PET were performed.

Table 1. Patient characteristics

Characteristics	Values
Age (y)	
Median	64
Range	21–85
Gender (*n*)	
Male (*n*)	18
Female (*n*)	14
RPA class	
III	3
IV	19
V	2
VI	8
Resection	
Gross total resection	16
Subtotal resection	10
Partial resection	6
Tumor location	
Frontal	9
Parietal	4
Temporal	12
Thalamus	1
Cerebellum	2
Basal ganglia	2
Two lobes	
Parieto-occipital	1
Temporo-occipital	1

Abbreviation: RPA = RTOG recursive partitioning analysis.

Imaging

Computed tomography was performed using helical CT equipment (Light Speed; General Electric, Waukesha, WI). Patients' heads were immobilized in a commercially available stereotactic mask, and scans were performed in 2.5-mm-thick slices without a gap.

Magnetic resonance imaging for radiation treatment planning was performed using 1.5-T equipment (Light Speed; General Electric, Waukesha, WI). Images were acquired using a standard head coil without rigid immobilization. Axial, three-dimensional gradient echo T_1-weighted sequences (matrix size, 256 × 256; field of view, 25 cm × 25 cm) with contrast medium (gadolinium-diethylenetriamine-pentacetic acid [Gd-DTPA; Magnevist, Schering, Berlin, Germany], 0.1 mmol/kg of body weight) at 2.0-mm slice thicknesses were acquired from the foramen magnum to the vertex, perpendicular to the main magnetic field. The T_2-weighted (2600/102 [effective]) images were acquired with a 512 × 224 matrix and a 24-cm field of view with a 6-mm-slice thickness.

The [^{11}C]MET-PET study was carried out using a standardized procedure. All patients fasted for at least 5 h before undergoing [^{11}C]MET-PET, and they were advised to have only a light breakfast on the morning of the examination day to ensure standardized metabolic conditions. The PET scanner used was an Advance NXi imaging system (General Electric Yokokawa Medical System, Hino-shi, Tokyo, Japan), which provides 35 transaxial images at 4.25-mm intervals. The crystal width is 4.0 mm (transaxial). The in-plane spatial resolution (full width at half-maximum) was 4.8 mm, and scans were performed in standard two-dimensional mode. Before the emission scans were performed, a 3-min transmission scan was performed to correct the photon attenuation, using a ring source containing 68 Ge. A dose of 7.0 MBq/kg [^{11}C]

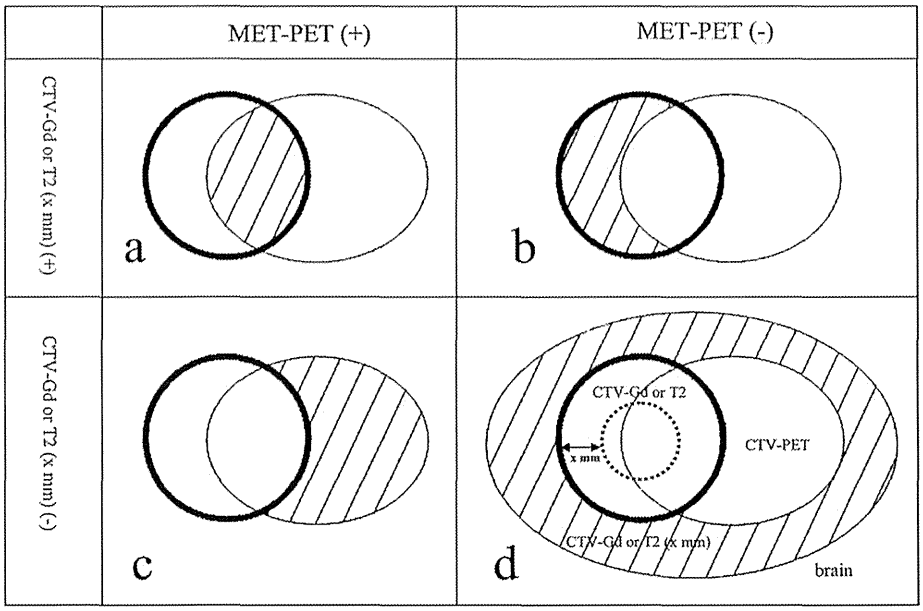

dotted line = CTV-Gd or T2, bold line= CTV-Gd or T2 (x cm), standard Line = CTV-PET

$$\text{Sensitivity} = \frac{a}{a+c} \qquad \text{Positive predictive value} = \frac{a}{a+b}$$

$$\text{Specificity} = \frac{d}{b+d} \qquad \text{Negative predictive value} = \frac{d}{c+d}$$

Fig. 1. We defined sensitivity, specificity, negative predictive value (NPV), and positive predictive value (PPV) by making comparison with the [^{11}C]MET-PET findings, which served as the gold standard in this study.

MET was injected intravenously, depending on the examination. Emission scans were acquired for 30 min, beginning 5 min after injection of [^{11}C]MET. During [^{11}C]MET-PET data acquisition, the patient's head position was continuously monitored using laser beams projected onto ink marks drawn over the forehead skin, and the head position was corrected as necessary.

Image registration was performed using Syntegra software (Philips Medical System, Fitchburg, WI) and a combination of automatic and manual methods. The quantitative accuracy of the mutual information registration was evaluated and approved by three observers, *i.e.*, a neurosurgeon, a radiation oncologist, and a nuclear medicine specialist.

Target volume delineation

The three observers delineated CTV using Gd-enhanced T_1-weighted MRI alone, T_2-weighted MRI alone, and [^{11}C]MET-PET alone, respectively. CTV volumes defined by [^{11}C]MET-PET, Gd-enhanced T_1-weighted MRI, and T_2-weighted MRI were delineated manually. Gd-enhanced T_1-weighted MRI CTV (CTV-Gd) was defined as the contrast-enhanced area on the Gd-enhanced T_1-weighted MRI, and the CTV-Gd (x mm) was defined as the x-mm (where x = 0-, 2-, 5-, 10-, and 20-mm) margin outside the CTV-Gd. The T_2-weighted MRI CTV (CTV-T_2) was defined as the high-intensity area on the T_2-weighted MRI, and we defined CTV-T_2 (x mm) as the x-mm (x = 0-, 2-, 5-, 10-, and 20-mm) margin outside the CTV-T_2 area (Fig. 1). The CTV-Gd (x-mm) and CTV-T_2 (x-mm) surfaces were then edited to limit expansion into adjacent skull. The [^{11}C]MET-PET CTV (CTV–[^{11}C]MET-PET) was defined as the area of accumulation of [^{11}C]MET, which was apparently higher than that in normal tissue on [^{11}C]MET-PET. The CTV– [^{11}C]MET-PET tumor/normal tissue index of 1.3 was considered the threshold for malignant activity. It is not clear which threshold value for the tumor/normal tissue index should become the reference value for determining GBM. For primary brain tumor, some reports have used 1.3 or 1.7 to determine the threshold value (12, 20). Although we used 1.3 as the threshold for tumor delineation in this study, the final determination of tumor delineation was obtained by consensus among three observers, and they did not necessarily adhere to a uniform threshold value of 1.3 for the tumor/normal tissue index. The same window parameters were used for all patients included in the trial.

Analysis

We defined sensitivity, specificity, negative predictive value (NPV), and positive predictive value (PPV) by making comparisons with the [^{11}C]MET-PET findings, which served as the gold standard in this study (Fig. 1). For statistical analyses, the statistical significance of the differences in the relationship between CTV-Gd (x mm) and CTV- [^{11}C]MET-PET and those of the relationship between CTV-T_2 (x mm) and CTV- [^{11}C]MET-PET were examined by using Tukey's test for multiple comparisons. A p value of <0.05 was considered statistically significant. We evaluated the validity of the margins by comparison with those reported in a study by Jansen et al. (19), which correlated results of histopathologic observations with CT/MR images.

RESULTS

The clinical characteristics and tumor locations of the 32 patients included in this study are given in Table 1. Patients